J. Braz. Chem. Soc., Vol. 14, No. 3, 388-395, 2003.
Printed in Brazil - ©2003 Sociedade Brasileira de Química
0103 - 5053 $6.00+0.00

Article

Chlorine Evolution Reaction at Ti/(RuO_2+Co_3O_4) Electrodes

Leonardo M. da Silva[a], Julien F. C. Boodts[a,b] and Luiz A. de Faria[*,b]

[a]*Departamento de Química, FFCLRP/Universidade de São Paulo, Av. Bandeirantes 3900, 14040-901 Ribeirão Preto - SP, Brazil*

[b]*Instituto de Química, Universidade Federal de Uberlândia, Campus Santa Mônica, Av. João Naves de Ávila 2160, 38400-902 Uberlândia - MG, Brazil*

A investigação do mecanismo eletródico e das propriedades eletrocatalíticas da reação de desprendimento de cloro, RDCl, foi executada em eletrodos mistos de óxido do tipo rutila e espinélio de composição nominal Ti/[RuO_2(x)+Co_3O_4(1-x)]. Os eletrodos foram preparados por decomposição térmica ($T_{calc.}$ = 470ºC; $t_{calc.}$ = 1h), com x variando entre 0 e 1 mudado em intervalos de 0,1. O estudo cinético foi executado registrando-se curvas corrente-potencial e pela determinação da ordem de reação com respeito aos íons H^+ e Cl^-. Um valor constante do coeficiente de Tafel de 33 mV foi obtido para concentrações de RuO_2 entre 0-80% mol, aumentando para 40 mV para concentrações superiores de RuO_2. Os dados experimentais apoiam o mecanismo de Erenburg e cols. para a RDCl. Um único mecanismo explica os resultados experimentais assumindo que o efeito "edge" influencie os valores do coeficiente de transferência eletrônica. A análise da atividade eletrocatalítica mostra que misturas de óxidos aumentam a atividade eletrocatalítica aparente.

A systematic investigation of the mechanistic and electrocatalytic properties of the chlorine evolution reaction, ClER, on mixed rutile/spinel oxides of nominal composition Ti/[RuO_2(x)+Co_3O_4(1-x)] was done. Electrodes were prepared using the thermal decomposition procedure ($T_{calc.}$ = 470ºC; $t_{calc.}$ = 1h), with x varied between 0 and 1, changed in 0.1 steps. Kinetics were studied recording quasi-stationary current-potential curves and reaction order determined with respect to H^+ and Cl^-. A constant Tafel slope of about 33 mV was found for the 0 – 80 mol% RuO_2 concentration interval, increasing to 40 mV for higher RuO_2 contents. Experimental data support the mechanism originally proposed by Erenburg *et al.* for the ClER. The edge effect exerts an influence on the electronic transfer coefficient values. Analysis of the electrocatalytic activity reveals an increase in the apparent electrocatalytic activity for the mixed oxides.

Keywords: cobalt, ruthenium, chlorine evolution, electrocatalytic activity

Introduction

Investigations of the chlorine evolution reaction, ClER, reveal this reaction is an "easy" one (low overpotential) characterised by a close to theoretical Tafel coefficient (30-40 mV).[1-4] Normally the ClER does not show a significant dependence on the nature of the electrode material.[1] However, the electrode kinetics can present a dependence on such parameters as the electrode morphology (*e.g.* roughness, porosity) and the electrolyte pH.[5]

The ClER is thermodynamically unfavoured (E^o = 1.36V(vs. RHE)) compared to the oxygen evolution reaction, OER, (E^o = 1.23V(vs. RHE)). However, chlorine can be produced from aqueous solutions with high current efficiency, especially at the lower pH-values of the electrolyte, due to the significant overpotential displayed by most electrode materials for the OER.[6] However, OER remains a side reaction during chlorine evolution, affecting directly the purity of the Cl_2 produced.[6,7] So, electrode selectivity for the ClER remains a problem of technological interest. Frequently[7-9] used additives to improve electrode stability and/or selectivity are TiO_2 and SnO_2.

A significant body of fundamental and applied research of the ClER is available. Most of these investigations are concerned with oxides (pure or mixtures) having the rutile structure[3,4,10-13] (*e.g.* RuO_2, PbO_2, TiO_2+RuO_2, IrO_2). The number of investigations of alternative materials of oxide mixtures possessing other crystallographic structures (*e.g.* rutile + spinel[14,15]) is rather scarce.

* e-mail: lafaria@ufu.br

Oxides having the spinel structure (*e.g.* Co_3O_4, $NiCo_2O_4$) have the advantage over the rutile oxides of being much cheaper. They present, however, the inconvenience of being unstable in acid medium:[16] an essential requirement for the ClER. A strategy to compatibilise the lower cost of the spinel oxides with their instability under acid conditions is the formation of mixed rutile + spinel oxides.[17-19]

Recent studies of the OER on Ti/[RuO_2+Co_3O_4] coatings by Da Silva *et al.*[17,20,21] showed these mixed oxides present interesting fundamental properties; stabilise the spinel under acid conditions and show an increase of the true electrocatalytic activity. Now we report the results of a detailed investigation of the kinetics and electrocatalytic properties of the Ti/[RuO_2+Co_3O_4] system for the ClER.

Experimental

Electrodes

Ti-supported electrodes of nominal composition Ti/[RuO_2(x)+Co_3O_4(1-x)], $0 \le x \le 1$, with x changed in steps of 0.1, were prepared by thermal decomposition (470 °C, 1h, in an air stream) of aqueous 0.2 mol dm^{-3} nitrate precursor mixtures. $Ru(NO_3)_3$ was prepared from $RuCl_3 \times xH_2O$ (Fluka) by precipitation of $Ru(OH)_3$ with NH_4OH. The precipitate, after abundant washing with cold water, was dissolved in concentrated HNO_3. Sandblasted Ti-supports (10x10x0.12 mm) were degreased with isopropanol and etched for 10 min. with boiling 10% oxalic acid. The precursor mixture was applied by brush to both faces of the Ti-support; the solvent evaporated at low temperature (80 - 90 °C) and the residue calcinated, in air, at 470 °C for 10 min in a pre-heated oven. This procedure was repeated until the desired oxide load was obtained (2.4 - 2.8 mg cm^{-2}, depending on composition). A final 1h annealing at the same temperature completed the treatment in all cases. In the case of the pure Co_3O_4 electrode a thin RuO_2 interlayer, prepared at 470 °C, was deposited between the Ti-support and the active layer. Such procedure improves the mechanical properties of the electrode. Electrodes were mounted in a Teflon holder as described earlier.[22]

The three-compartment cell used has been described previously.[22] Ohmic drop was minimised using a Luggin capillary approaching the electrode from below while two, heavily platinised, platinum counter electrodes ensured uniformity of the current on the two opposite faces of the samples. Electrode potentials were read against a sodium saturated calomel electrode (SSCE).

Solutions, methods and equipment

$Ru(NO_3)_3$ and $Co(NO_3)_2$ (Aldrich) precursor solutions (0.2 mol dm^{-3}) were prepared using Milli-Q quality water ($R \ge 18.6 M\Omega$). Precursor mixtures were prepared mixing the appropriate volumes of precursor solutions to obtain the desired nominal composition.

In situ surface characterisation and electrode kinetics were determined using as supporting electrolyte 5.0 mol dm^{-3} NaCl + 0.01 mol dm^{-3} HCl. The order of reaction with respect to Cl^-, ς_{Cl^-}, was determined covering the 0.5-5.0 mol dm^{-3} NaCl concentration interval keeping the ionic strength constant by substitution of NaCl with $NaClO_4$ maintaining the pH at 2. The order of reaction with respect to H^+, ς_{H^+}, was obtained changing the $[H^+]$ between 0.1 and 0.01 by partial substitution of NaCl with HCl.

PAR instrumentation was used throughout. Voltammetric curves were recorded at 20 mV s^{-1} covering the 0.0–1.0 V(vs. SSCE) potential interval. The voltammetric charge spent in this potential range was determined by integration of the anodic, q_a, or cathodic, q_c, branch of the *j* vs. *E* curve using PAR software (M-270).

Potentiostatic curves recorded under quasi-stationary conditions were obtained keeping, initially, the electrode potential at 0.9 V(vs. SSCE) for 15 min, then moving the potential anodically, at 56 μV s^{-1}, until the current reached a value of approximately 100 mA.

Reaction orders were determined by conditioning the electrode at 0.9 V(vs. SSCE) during 5 min, then stepping the potential to the selected value (E = 1.08 V(vs. SSCE)) when the *j* vs. *t*-curves were recorded during 15 min. All electrodes were processed in the same solution before changing the NaCl concentration.

Solutions were deaerated before and heavily stirred during each experiment using a strong nitrogen flux (99.995% purity).

Results and Discussion

Voltammetric curves

Voltammetric curves, *E* vs. *j*, were recorded to monitor *in situ* the surface state of the electrodes.[7] Curves were recorded between 0.0-1.0V(vs. SSCE) (potential range where only double layer charging and solid state surface redox transitions take place). Figure 1 shows representative stationary voltammetric profiles recorded before the kinetic experiments.

The CV profile of the Ti/Co_3O_4 electrode (Figure 1A) presents a band in the 0.6-0.8 V(vs. SSCE) potential interval which has been attributed to the Co(II)/Co(III) solid state surface transition.[20] As shown in Figure 1B, representative of the mixed oxides and the Ti/RuO_2 electrode, the introduction of RuO_2 causes a significant increase in the current density. The intense cathodic current presented by

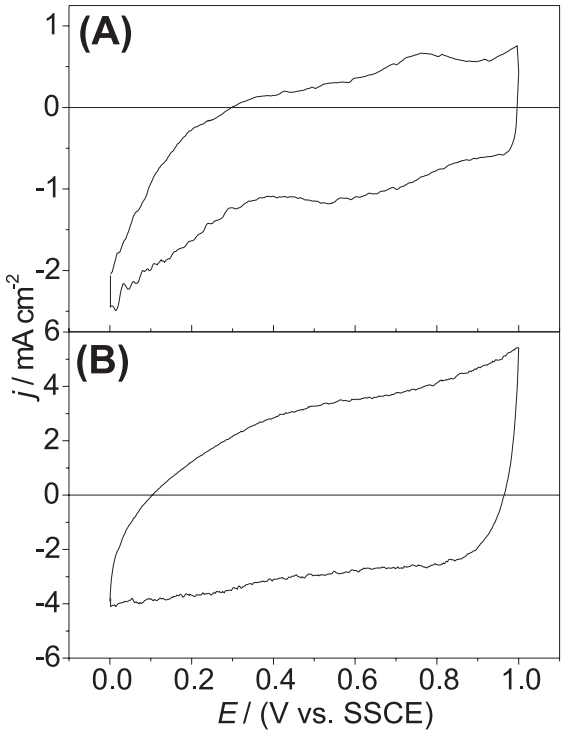

Figure 1. Voltammetric curves of Ti/[RuO_2(x)+Co_3O_4(1-x)]: (A) x = 0; (B) x = 0.5. Supporting electrolyte: 5.0 mol dm^{-3} NaCl + 0.01 mol dm^{-3} HCl. T = 24 °C.

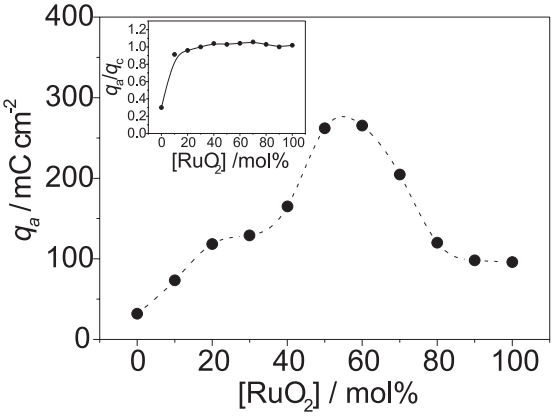

Figure 2. Dependence of q_a on nominal electrode composition. Supporting electrolyte: 5.0 mol dm^{-3} NaCl + 0.01 mol dm^{-3} HCl. T = 24 °C.

the Ti/Co_3O_4 electrode disappears from the CV when [RuO_2] ≥ 10mol%.

The anodic voltammetric charge, q_a, obtained by integration of the anodic branch of the E vs. j plots, is a parameter proportional to the active surface sites.[7] Figure 2 shows the dependence of q_a on nominal electrode composition. q_a is seen to increase strongly with the introduction of RuO_2 into the coating, reaching a maximum at 50-70 mol% nominal RuO_2 content. Such behavior is in good agreement with previous work conduced by Da Silva *et al.*[20,21] who reported for sulfuric acid solution a maximum in q_a and differential capacity values, for the same interval of nominal composition.

Except for the Ti/Co_3O_4 electrode, all other coatings presented a q_a/q_c-value close to one (see inset Figure 2). This finding indicates reversibility of the solid state surface redox transitions in slightly acid chloride medium. The q_a/q_c ratio for the Ti/Co_3O_4 electrode, obtained by integration of the 0.3-1.0V(vs. SSCE) potential interval, was 0.3 and denounces the existence of an uncompensated cathodic process during the potential sweep. As proposed by Da Silva *et al.*[20], this uncompensated cathodic process observed during continuous potential cyclisation in acid medium is due to CoO dissolution according to the following processes:

Electrode reactions:

$$2\,CoO + Co_2O_3 + H_2O \Rightarrow 2\,Co_2O_3 + 2\,e^- + 2\,H^+ \quad \text{(anodic scan)} \qquad (1)$$

$$2\,Co_2O_3 + 4\,e^- + 4\,H^+ \Rightarrow 4\,CoO + 2\,H_2O \quad \text{(cathodic scan)} \qquad (2)$$

Dissolution process:

$$CoO_{(s)} + H_2O + Co(OH)_{2(s)} + 2\,H^+ \Rightarrow Co^{2+}{}_{(aq)} + 2\,H_2O \qquad (3)$$

In agreement with previous results obtained in sulfuric acid solution[20] the absence of the intense cathodic current in the j/E profiles (see Figure 1B) of the mixed rutile/spinel oxides supports the introduction of RuO_2 stabilizes the coatings in slightly acidified chloride medium.

Tafel lines

For each electrode two sets of current-potential curves were recorded without interruption (each set is made up of a forward and backward potential scan). Hysteresis between scans was negligible. All experimental Tafel curves showed, at high overpotentials, a deviation from linearity, requiring correction for ohmic drop, IR, in order to permit an appropriate interpretation. E vs. log j curves, already corrected for IR, representative of the behaviour of the system, are shown in Figure 3.

The influence of ohmic drop on the polarisation curve can be written as:

$$E - IR = a + b\log j, \qquad (4)$$

where R is the total ohmic resistance, E is the electrode potential, a is a constant and b is the Tafel slope. The best

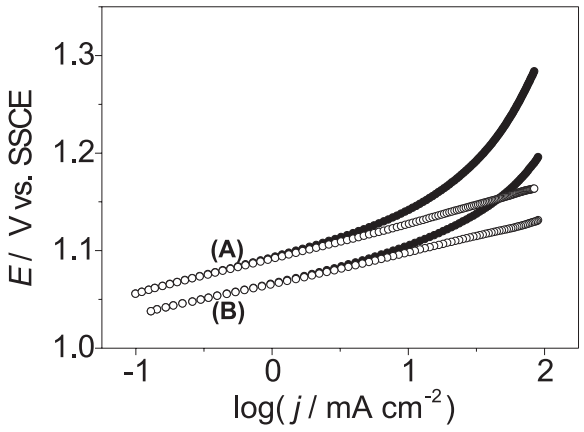

Figure 3. Tafel plots for ClER at Ti/[RuO_2(x)+Co_3O_4(1-x)]: (A) x = 0; (B) x = 0.5. (●) Raw data. (○) After correction for *IR*. Supporting electrolyte: 5.0 mol dm^{-3} NaCl + 0.01 mol dm^{-3} HCl. T = 24 °C.

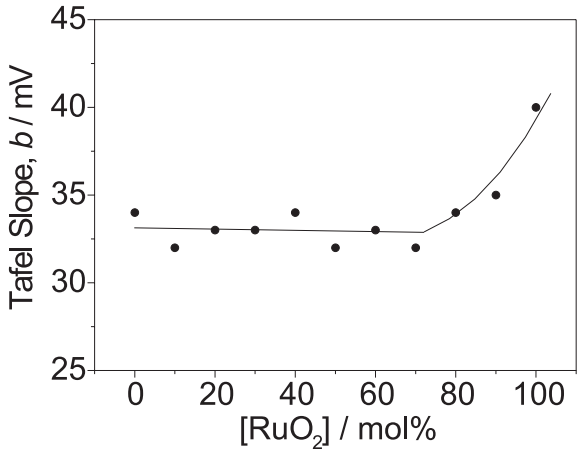

Figure 4. Tafel slope, *b*, as a function of oxide composition.

R-value is obtained when a perfect linearisation of equation 4 is verified (see Figure 3). The experimental data to be used in the linearisation procedure are the ones localised in the high overpotential domain where the influence of ohmic drop is more pronounced. The criterion used to determine the best linearisation of the curve is based on the correlation coefficient of the high current data. The *IR* correction of the curves was done following the procedure initially proposed by Shub and Reznik.[23] As described previously by us,[17] an easy way to determine the optimum *R*-value is by changing the approximate value in increments of 0.01Ω using the Origin (version 5.0) software until the best correlation coefficient is obtained.

R-values in the range of 0.23-1.43 were obtained which are in good agreement with similar systems made up of thin (~3 μm) metallic conductive coatings.[17,24-26] These investigations also show that for this kind of electrode material the main contribution to the total resistance of the system comes from the solution resistance between the working electrode and the Luggin capillary.

Independent of coating composition, after correction of the Tafel curves for *IR*-drop, a single linear segment is obtained (see Figure 3) showing deviation from linearity of the raw data is only due to uncompensated resistance or-be-it the kinetics of the ClER are independent of potential. This behaviour is rather different from the OER, for which a strong dependence on potential and nominal electrode composition was observed,[17] showing the ClER is a much less complex electrode process.

Figure 3 also shows that the substitution of Co_3O_4 by RuO_2 improves the global activity of the electrode decreasing significantly the ClER overpotential.

Figure 4 shows the dependence of the Tafel coefficient, *b*, on nominal oxide composition.

With the exception of pure RuO_2, for which b = 40 mV, the Tafel coefficient is independent of composition showing a value close to 33 mV. The *b*-values for pure RuO_2 and Co_3O_4 are in good agreement with the literature.[1,2]

Reaction orders with respect to Cl^- and H^+ ions.

The Tafel slope data obtained in this work can be interpreted on the basis of several different electrode mechanisms.[2,3] So, the reaction order becomes the crucial factor to discriminate between the various possibilities.

Keeping the electrode potential, *E*, and all concentrations [*w*]'s, constant, except the concentration of the species of interest, [*S*], and attending the criterion for the high field approximation ($\eta \geq 0.1$V), the reaction order with respect to *S*, ζ_S, can be calculated from:

$$\zeta_S = (\partial \log j / \partial \log[S])_{E,[w]\neq S} \quad (5)$$

To propose an electrode mechanism for the ClER two reaction orders must be determined: (i) with respect to Cl^- at constant pH and (ii) with respect to H^+ at constant Cl^- concentration. In both cases the ionic strength of the solution should be kept constant to avoid diffuse double layer effects.[3]

Figure 5 shows representative log *j* vs. log[Cl^-] profiles. *j*-values were read at 1.08V(vs. SSCE). It is worthwhile to mention that E = 1.08V(vs. SSCE) does not attend the theoretical criterion for the high field approximation. However, the experimental conditions employed are far from the standard condition ([Cl^-] = 1.0 mol dm^{-3} and p_{Cl_2} = 1 bar). Indeed, the chloride concentration used was between 0.5 and 5.0 mol dm^{-3} and, even more important, the experiment was carried out under heavily stirred conditions so that $p_{Cl_2} << 1$ bar.

The fact an excellent linearity of the log *j* vs. log [Cl^-] was observed (r = 0.998) validates the high field approximation from an experimental point of view. The slope of the lines is independent of electrode composition, presenting values scattered around unity (0.95-1.10). Such results reveals a positive influence of the [Cl^-] on the rate of the ClER.

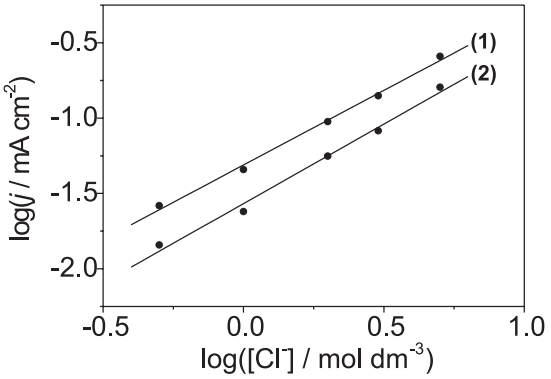

Figure 5. Dependence of current density, *j*, on [Cl^-] at Ti/[RuO_2(x)+Co_3O_4(1-x)]: (1) x = 1; (2) x = 0. $j_{measured}$: 1.08 V(vs. SSCE). Supporting electrolyte: 5.0 mol dm^{-3} ([NaCl] + [$NaClO_4$]) + 10^{-2} mol dm^{-3} HCl.

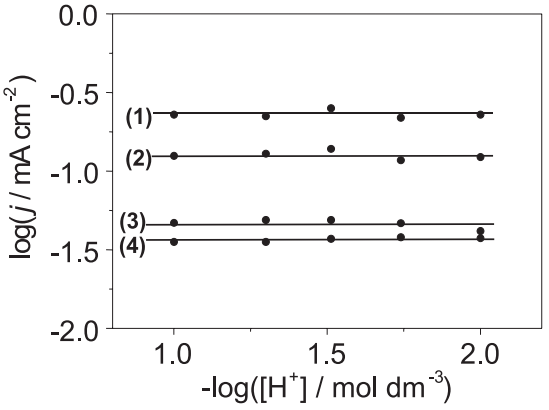

Figure 6. Dependence of current density, *j*, on pH at Ti/[RuO_2(x)+Co_3O_4(1-x)]: (1) x = 1; (2) x = 0.5; (3) x = 0.2; (4) x = 0. $j_{measured}$: 1.08 V(vs. SSCE). Supporting electrolyte: 5.0 mol dm^{-3} (NaCl + HCl).

Figure 6 shows representative plots of the influence of pH on the current measured at 1.08 V(vs. SSCE). The HCl concentration was varied between 0.01 and 0.1 mol dm^{-3} while the ionic strength was kept constant at 5 mol dm^{-3} (NaCl + HCl). Good linearity was obtained for all electrodes investigated (r = 0.998). Although no influence of the solution acidity on the ClER is expected on the basis of purely thermodynamic considerations,[3] some literature reports,[2-4] investigating different oxide materials, report the reaction rate is sometimes depressed by increasing acidity. However, in the case of the title system, as shown in Figure 6, no significant influence of the pH on the ClER rate is observed. The reaction order with respect to H^+ was found to be independent on oxide composition presenting values close to zero. As reported by Consonni *et al.*[3] the influence of pH on the ClER is dependent on the peculiarities of the oxide/solution interface (*e.g.* crystallographic nature of the oxide). So, the independence of the ClER on pH, found by us for the Co_3O_4+ RuO_2 system, is probably due to the crystallographic structure of these oxides.

Reaction mechanism

Several different electrode mechanisms have been proposed for the ClER.[1-3] Considering the experimental *b*-values and reaction orders with respect to H^+ and Cl^- ions, the mechanism proposed by Erenburg *et al.*[27] adequately describes the electrode reaction:

b/mV (T = 24 °C; $\alpha = 0.5$)

$\equiv S + Cl^- \rightarrow \equiv S—Cl + e^-$	120	(a)
$\equiv S—Cl \rightarrow \equiv S—Cl^+ + e^-$	40	(b)
$\equiv S—Cl^+ + Cl^- \rightarrow \equiv S + Cl_2$	30	(c)

where ≡S represents an active surface site.

In agreement with the experimental ζ_{H^+}-value of zero, the above mechanism does not predict any dependency of the reaction rate on pH. Considering steps (b) or (c) as the rate determining step, rds, reaction orders with respect to Cl^- of 1 or 2 are predicted, respectively.

Considering step (c) as the rds, in which case an order of reaction with respect to chloride of two is theoretically predicted, is not consistent with the experimental $\zeta_{Cl^-} = 1$ value.

Considering the experimental reaction order with respect to Cl^- and taking step (b) as rds, the reaction rate, *j*, at $\eta \geq 0.1$V can be written as:

$$j = k[Cl^-] \exp\{[(1+\alpha)F(E-E^\circ)]/R \cdot T\} \quad (6)$$

Rearranging and applying the definition $b \equiv (\partial E/\partial \log j)_T$, the theoretical Tafel slope is given by:

$$b = 2.302 \cdot R \cdot T / [F(1+\alpha)] \quad (7)$$

Equation 7 does not take into account the influence of the electrode morphology on electrode kinetics. However, contrary to the OER[17] the ClER is considered an "easy"

electrode process showing almost no dependence on the electronic nature and morphology of the electrode material[1] suggesting the influence of the porous/rugged electrode microstructure is rather small. Besides, under conditions of intense gas evolution, the microstructure rapidly becomes clogged by gas bubbles as a result of which only the more external surface is active. As a result the oxide/solution interface approaches the behaviour of a planar electrode.

According to equation 7, Tafel coefficients of 30 and 40 mV (T = 24 °C) require the electronic transfer coefficient, *a*, to assume values of 1.0 e 0.5, respectively. From a theoretical point of view α = 0.5 represents a perfect symmetry between the activation energy curves with respect to oxidised and reduced species, while α = 1 represents an electron transfer occurring without activation in the electric component of the total activation energy barrier.[6,28] According to Krishtalik[29] a value of α = 1 is not necessarily associated with the complete disappearance of the energy barrier (this process may be called quasibarrierless), and can be predicted on the basis of the quantum mechanical theory of an elementary act. It was shown that certain reactions, particularly the ClER, are, in fact, quasibarrierless.[30]

Since α, is an intrinsic characteristic of the given charge-transfer reaction at a particular interface,[31] changes in the α-value can be used to correlate the influence of the electrode material on the electron transfer process. Figure 7 shows the dependence of α on nominal electrode composition. α-values were calculated substituting the experimental *b*-value (see Figure 4) in equation 7 taking T = 24 °C.

As shown in Figure 7, α-values increase with decreasing RuO_2-content reaching a constant value of ~0.8 for [RuO_2] ≤ 70 mol%. This result, in principle, suggests that the nominal electrode composition affects the magnitude of the activation barrier of step (b), considered the rds. So, α can be correlated with the change in ≡S—Cl bond strength. This change can find its origin in several effects: (i) change in the [Ru]/[Co] surface concentration with changing composition; (ii) interaction at the electronic level (synergetic effects) between the surface Co and Ru-sites; (iii) influence of the oxide morphology on the distribution of the surface electric filed causing a modification in the nature of the active sites (edge effect).

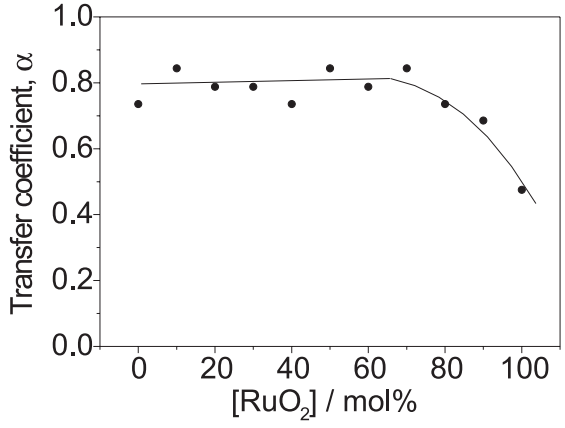

Figure 7. Dependence of the electronic transfer coefficient, α, on the nominal electrode composition.

In a earlier paper[20] Ru-surface enrichment for [RuO_2] ≥ 10 mol% has been shown to occur. As a result surface electrochemistry in the mixed coatings is governed by Ru-sites. This experimental evidence suggests that the possible contribution of steps (i) and (ii) in the change in the α-value is minimised. So, despite the ClER being considered an external surface reaction[7] (occurs mainly at the surface of the more external oxide region), the change in α shown in Figure 7 can be attributed mainly to the dependence of the edge effect on the oxide morphology (effect iii). This is consistent with previous results which showed that the interaction between the rutile (RuO_2) and spinel (Co_3O_4) structures varies with oxide composition, modifying the degree of crystallinity and the morphology of the mixed oxides.[20]

This discussion is consistent with the proposals of Consonni *et al.*[3] for the ClER. These authors support that despite the fact the ClER is an electrode process that is little affected by the chemical nature of the electrode material, its electrode kinetics can be influenced by the electrode morphology (roughness/porosity) and the pH of the electrolyte.

Analysis of the electrocatalytic activity

Electrocatalytic activity depends on both electronic and geometric factors. Since the voltammetric charge (*i.e.* the active surface area) is a function of the oxide composition, true electrocatalytic effects can be found normalising the current for the voltammetric charge.[7] Figure 8 shows a plot of the apparent, *j*, and true electrocatalytic activity, j/q_a, measured at 1.08 V(vs. SSCE) as function of nominal oxide composition. q_a-values were extracted from Figure 2 and *j*-values were obtained from Tafel plots.

Figure 8A shows maximum apparent electrocatalytic activity for the ClER is observed in the 50-100 mol% RuO_2 range, differently from the OER for which maximum apparent and true electrocatalytic activity is observed in the 20-40 mol% RuO_2 range.[17] These results support that the more active electrodes for the ClER are the least active

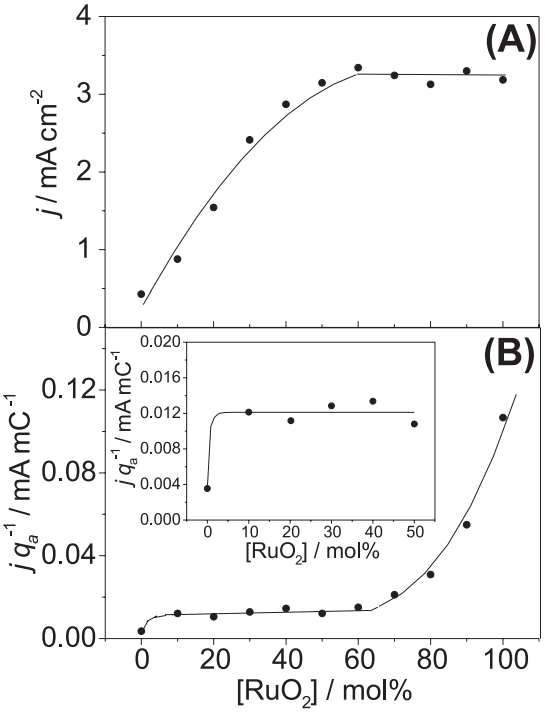

Figure 8. Current density, j, (A) and normalised current density, j/q_a, (B) as function of nominal electrode composition for ClER. 5.0 mol.dm^{-3} NaCl + 0.01 mol.dm^{-3} HCl solution. j-values were extracted from Tafel plots. Inset: magnification of the 10-50 mol% RuO_2 range.

for the OER, supporting coating with 50-100 mol% RuO_2 contents present a better selectivity for chlorine production.

The inset in Figure 8B shows a sudden increase in j/q_a-ratio with the introduction of only 10mol% RuO_2. This finding is in good agreement with results reported by Shalaginov *et al.*[15], who found that doping titanium-supported cobalt oxide films (Co_3O_4) with small amounts of ruthenium leads to a significant increase of the electrocatalytic activity for ClER. These authors also observed, for identical electrolysis conditions, that doped titanium-supported cobalt oxide electrodes ([Ru] ≅ 2.5 atom%) is not inferior in its electrochemical activity and selectivity with respect to ClER than the well-known DSA® of optimum composition (RuO_2(30 mol%) + TiO_2(70 mol%)).

Figure 8B shows that in the 10mol% ≤ [RuO_2] ≤ 50 mol% composition range the true electrocatalytic activity remains constant. According to the literature[7] this behaviour indicates the occurrence of surface enrichment with Ru, as indeed was observed by us in the *in situ* and *ex situ* characterisation studies reported earlier for this electrode system.[20] In accordance with previous discussion (see previous section), the steep increase in j/q_a-ratio presented for [RuO_2] ≥ 60 mol%, can be correlated with modifications in electrode morphology. Such behaviour according to XRD-data[20] indicates increasing crystallinity, and reducing roughness, resulting in an oxide surface intrinsically more active for ClER.

The very different behaviour observed for ClER (Figures 8A and 8B), as compared to OER investigated earlier[17] shows the electrocatalytic pattern for ClER differs considerably from that for OER, showing that the manifestation of synergetic effects by mixed oxides, as indeed observed for OER, also depends on the nature of the electrode reaction.[7] Comparison between Figures 8A and 8B reveals the increase in the apparent electrocatalytic activity presented by mixed oxides is mainly due to morphological aspects (high degree of roughness and/or porosity). Therefore, electronic effects (synergism) present a minor contribution to the electrocatalytic activity of the mixed oxides.

Conclusions

The replacement of Co_3O_4 by RuO_2 results in electrode materials having a higher electrode surface area when compared to pure oxides. A maximum value of the surface area is observed for 50 mol% ≤ [RuO_2] ≤ 70 mol%. For the exploited potential range and all electrode compositions investigated, the ClER kinetics on Ti/(RuO_2+Co_3O_4) are governed by a single rate determining step. Contrary to the Cl^--anions, H^+ doesn't exert influence on the electrode kinetics. Experimental data support the electrode mechanism proposed by Erenburg *et al.* for the ClER. Modification in the nature of the active surface sites due to changes in the electrode morphology cause a dependence of α-values (0.5-0.80) on nominal electrode composition. Analysis of the electrocatalytic activity shows the main contribution to the global electrocatalytic (geometric and electronic effects) presented by mixed oxides comes from geometric effects (*e.g.* roughness, porosity).

Acknowledgements

L.M. Da Silva wishes to thank a MSc Fellowship received from the CAPES Foundation. J.F.C. Boodts and L.A. De Faria wish to thank financial support received from the CAPES/FAPEMIG/CNPq Foundations. J.F.C. Boodts acknowledges a Visiting Researcher Fellowship granted by the CNPq.

References

1. Trasatti, S.; Lodi, G. In *Electrodes of Conductive Metallic Oxides*; Trasatti, S., ed. Elsevier: Amsterdam, 1981, Chap. 10.
2. Boggio, R.; Carugati, A.; Lodi, G.; Trasatti, S; *J. Appl. Electrochem.* **1985**, *15*, 335.

3. Consonni, V.; Trasatti, S.; Pollak, F.; O'Grady, W.E.; *J. Electroanal. Chem*. **1987**, *228*, 393.
4. De Faria, L.A.; Boodts, J.F.C.; Trasatti, S.; *Electrochim. Acta* **1997**, *42*, 3525.
5. Trasatti, S.; *Electrochim. Acta* **1987**, *32*, 369.
6. Trasatti, S; Lodi, G. In *Electrodes of Conductive Metallic Oxides*; Trasatti, S., ed. Elsevier: Amsterdam, 1981, Part B, p. 535.
7. Trasatti, S.; *Electrochim. Acta* **1991**, *36*, 225.
8. Iwakura, C.; Inai, M.; Uemura, T.; Tamura, H.; *Electrochim. Acta* **1981**, *26*, 579.
9. Spasojevic, M.; Krstajic, N.; Jaksic, M.; *J. Res. Inst. Catalysis* **1984**, *32*, 29.
10. Arikado, T.; Iwakura, C.; Tamura, H.; *Electrochim. Acta* **1978**, *23*, 9.
11. Bondar, U.; Borisova, A.A.; Kalinovskii, E.A.; *Élektrokhimiya* **1977**, *13*, 1540.
12. Janssen, L.J.J.; Starmans, L.M.C.; Visser, J.G.; Barendrecht, E.; *Electrohim. Acta* **1977**, *22*, 1093.
13. Mráz, R.; Srb, V.; Tichý, S.; *Electrochim. Acta* **1973**, *18*, 551.
14. Shub, D.M.; Reznik, M.F.; Shalaginov, V.V.; *Élektrokhimiya* **1985**, *21*, 937.
15. Shalaginov, V.V.; Markina, O.V.; Shub, D.M.; *Élektrokhimiya* **1980**, *16*, 271.
16. Shub, D.M.; Chemodanov, A.N.; Shalaginov, V.V.; *Élektrokhimiya* **1978**, *14*, 595.
17. Da Silva, L.M.; Boodts, J.F.C.; De Faria, L.A.; *Electrochim. Acta* **2001**, *46*, 1369.
18. Krstajíc, N.; Trasatti, S.; *J. Electrochem. Soc*. **1995**, *142*, 2675.
19. De Faria, L.A.; Boodts, J.F.C.; Trasatti, S.; *Electrochim. Acta* **1992**, *37*, 2511.
20. Da Silva, L.M.; Boodts, J.F.C.; De Faria, L.A.; *Electrochim. Acta* **2000**, *45*, 2719.
21. Da Silva, L.M.; De Faria, L.A.; Boodts, J.F.C.; *J. Electroanal. Chem*. **2002**, *532*,141.
22. Garavaglia, R.; Mari, C.M.; Trasatti, S.; *J. Appl. Electrochem*. **1978**, *8*, 135.
23. Shub, D.M.; Reznik, M.F.; *Élektrokhimiya* **1985**, *21*, 855.
24. Da Silva, L.M.; De Faria, L.A.; Boodts, J.F.C.; *Pure Appl. Chem*. **2001**, *73*, 1871.
25. da Silva, L.A.; Alves, V.A.; da Silva, M.A.P.; Trasatti, S.; Boodts, J.F.C.; *Can. J. Chem*. **1997**, *75*, 1483.
26. De Faria, L.A.; Boodts, J.F.C.; Trasatti, S.; *J. Appl. Electrochem*. **1996**, *26*, 1195.
27. Erenburg, R.G.; Krishtalik, L.I.; Yaroshevskaya, I.P.; *Élektrokhimiya* **1975**, *11*, 1236.
28. Bard, A.J.; Faulkner, L.R.; *Electrochemical Methods: Fundamentals and Applications*, John Wiley and Sons: New York, 1980, p. 96.
29. Krishtalik, L.I. In *Comprehensive Treatise of Electrochemistry*; Bockris, J.O'M.; Conway, B.E.; Yeager, E.; White, R.E., eds.; Kluwer Academic/Plenum: The Netherlands, 1981, p. 126, Vol. 7.
30. Krishtalik, L.I.; *Electrochim. Acta* **1968**, *13*, 1045.
31. Bockris, J.O'M.; Reddy, A.KN.; *Modern Electrochemistry*; Plenum Press: New York, N.Y, 1977, p. 918.

Received: July 29, 2002
Published on the web: April 28, 2003

FAPESP helped in meeting the publication costs of this article.